

# Spatial Deep Learning for Wireless Scheduling

Wei Cui, Kaiming Shen, *Student Member, IEEE*, and Wei Yu, *Fellow, IEEE*

**Abstract**—The optimal scheduling of interfering links in a dense wireless network with full frequency reuse is a challenging task. The traditional method involves first estimating all the interfering channel strengths then optimizing the scheduling based on the model. This model-based method is however resource intensive and computationally hard, because channel estimation is expensive in dense networks; further, finding even a locally optimal solution of the resulting optimization problem may be computationally complex. This paper shows that by using a deep learning approach, it is possible to bypass channel estimation and to schedule links efficiently based solely on the geographic locations of transmitters and receivers for networks in which the channels are largely functions of distance dependent path-losses. This is accomplished by unsupervised training over randomly deployed networks, and by using a novel neural network architecture that takes the geographic spatial convolutions of the interfering or interfered neighboring nodes as input over multiple feedback stages to learn the optimum solution. The resulting neural network gives near-optimal performance for sum-rate maximization and is capable of generalizing to larger deployment areas and to deployments of different link densities. Moreover, to provide fairness, this paper proposes a novel scheduling approach that utilizes the sum-rate optimal scheduling algorithm over judiciously chosen subsets of links for maximizing a proportional fairness objective over the network. The proposed approach shows highly competitive and generalizable network utility maximization results.

**Index Terms**—Deep learning, discrete optimization, geographic location, proportional fairness, scheduling, spatial convolution

## I. INTRODUCTION

Scheduling of interfering links is one of the most fundamental tasks in wireless networking. Consider a densely deployed device-to-device (D2D) network with full frequency reuse, in which nearby links produce significant interference for each other whenever they are simultaneously activated. The task of scheduling amounts to judiciously activating a *subset* of mutually “compatible” links so as to avoid excessive interference for maximizing a network utility.

The traditional approach to link scheduling is based on the paradigm of first estimating the interfering channels (or at least the interference graph topology), then

optimizing the schedule based on the estimated channels. This model-based approach, however, suffers from two key shortcomings. First, the need to estimate not only the direct channels but also all the interfering channels is resource intensive. In a network of  $N$  transmitter-receiver pairs,  $N^2$  channels need to be estimated within each coherence block. Training takes valuable resources away from the actual data transmissions; further, pilot contamination is inevitable in large networks. Second, the achievable data rates in an interfering environment are nonconvex functions of the transmit powers. Moreover, scheduling variables are binary. Hence, even with full channel knowledge, the optimization of scheduling is a nonconvex integer programming problem for which finding an optimal solution is computationally complex and is challenging for real-time implementation.

This paper proposes a new approach, named *spatial learning*, to address the above two issues. Our key idea is to recognize that in many deployment scenarios, the optimal link scheduling does not necessarily require the exact channel estimates, and further the interference pattern in a network is to a large extent determined by the relative locations of the transmitters and receivers. Hence, it ought to be possible to *learn* the optimal scheduling based solely on the geographical locations of the neighboring transmitters/receivers, thus bypassing channel estimation altogether. Toward this end, this paper proposes a neural network architecture that takes the geographic spatial convolution of the interfering or interfered neighboring transmitters/receivers as input, and learns the optimal scheduling in a densely deployed D2D network over multiple stages based on the spatial parameters alone.

We are inspired by the recent explosion of successful applications of machine learning techniques [1], [2] that demonstrate the ability of deep neural networks to learn rich patterns and to approximate arbitrary function mappings [3]. We further take advantage of the recent progress on fractional programming methods for link scheduling [4]–[6] that allows us to compare against the state-of-the-art benchmark. The main contribution of this paper is a specifically designed neural network architecture that facilitates the spatial learning of geographical locations of interfering or interfered nodes and is capable of achieving a large portion of the optimum sum rate of the state-of-the-art algorithm in a computationally efficient manner, while requiring no explicit channel state information (CSI).

Traditional approach to scheduling over wireless interfering links for sum rate maximization are all based on (non-convex) optimization, e.g., greedy heuristic search

Manuscript submitted to IEEE Journal on Selected Areas in Communications on July 21, 2018, revised October 15, 2021. This work is supported by Natural Science and Engineering Research Council (NSERC) via the Canada Research Chairs program. The materials in this paper have been presented in part at the IEEE Global Communication Conference (GlobeCom), Abu Dhabi, December 2018. The authors are with The Edward S. Rogers Sr. Department of Electrical and Computer Engineering, University of Toronto, Toronto, ON M5S 3G4, Canada (e-mails: {cuiwei2, kshen, weiyu}@ece.utoronto.ca).

[7], iterative methods for achieving quality local optimum [4], [8], methods based on information theory considerations [9], [10] or hyper-graph coloring [11], [12], or methods for achieving the global optimum but with worst-case exponential complexity such as polyblock-based optimization [13] or nonlinear column generation [14]. The recent re-emergence of machine learning has motivated the use of neural networks for wireless network optimization. This paper is most closely related to the recent work of [15], [16] in adapting deep learning to perform power control and [17] in utilizing ensemble learning to solve a closely related problem, but we go one step further than [15]–[17] in that we forgo the traditional requirement of CSI for spectrum optimization. We demonstrate that in wireless networks for which the channel gains largely depend on the path-losses, the location information (which can be easily obtained via global positioning system) can be effectively used as a proxy for obtaining near-optimum solution, thus opening the door for much wider application of learning theory to resource allocation problems in wireless networking.

The rest of the paper is organized as follows. Section II establishes the system model. Section III proposes a deep learning based approach for wireless link scheduling for sum-rate maximization. The performance of the proposed method is provided in Section IV. Section V discusses how to adapt the proposed method for proportionally fair scheduling. Conclusions are drawn in Section VI.

## II. WIRELESS LINK SCHEDULING

Consider a scenario of  $N$  independent D2D links located in a two-dimensional region. The transmitter-receiver distance can vary from links to links. We use  $p_i$  to denote the fixed transmit power level of the  $i$ th link, if it is activated. Moreover, we use  $h_{ij} \in \mathbb{C}$  to denote the channel from the transmitter of the  $j$ th link to the receiver of the  $i$ th link, and use  $\sigma^2$  to denote the background noise power level. Scheduling occurs in a time slotted fashion. In each time slot, let  $x_i \in \{0, 1\}$  be an indicator variable for each link  $i$ , which equals to 1 if the link is scheduled and 0 otherwise. We assume full frequency reuse with bandwidth  $W$ . Given a set of scheduling decisions  $x_i$ , the achievable rate  $R_i$  for link  $i$  in the time slot can be computed as

$$R_i = W \log \left( 1 + \frac{|h_{ii}|^2 p_i x_i}{\Gamma (\sum_{j \neq i} |h_{ij}|^2 p_j x_j + \sigma^2)} \right), \quad (1)$$

where  $\Gamma$  is the SNR gap to the information theoretical channel capacity, due to the use of practical coding and modulation for the linear Gaussian channel [18]. Because of the interference between the links, activating all the links at the same time would yield poor data rates. The wireless link scheduling problem is that of selecting a subset of links to activate in any given transmission period so as to maximize some network utility function of the achieved rates.

This paper considers the objective function of maximizing the weighted sum rate over the  $N$  users over each scheduling slot. More specifically, for fixed values of weights  $w_i$ , the scheduling problem is formulated as

$$\underset{\mathbf{x}}{\text{maximize}} \quad \sum_{i=1}^N w_i R_i \quad (2a)$$

$$\text{subject to} \quad x_i \in \{0, 1\}, \forall i. \quad (2b)$$

The weights  $w_i$  indicate the priorities assigned to each user, (i.e., the higher priority users are more likely to be scheduled). The overall problem is a challenging discrete optimization problem, due to the complicated interactions between different links through the interference terms in the signal-to-interference-and-noise (SINR) expressions, and the different priority weights each user may have.

The paper begins by treating the scheduling problem with equal weights  $w_1 = w_2 = \dots = w_N$ , equivalent to a sum-rate maximization problem. The second part of this paper deals with the more challenging problem of scheduling under adaptive weights  $w_1, w_2, \dots, w_N$  for maximizing a network utility. The assignment of weights is typically based on upper-layer considerations, e.g., as function of the queue length in order to minimize delay or to stabilize the queues [19], or as function of the long-term average rate of each user in order to provide fairness across the network [20], or as combination of both.

This paper utilizes unsupervised training to optimize the parameters of the neural network. The results will be compared against multiple benchmarks including a recently developed and the-state-of-art fractional programming approach (referred to as FPLinQ or FP) [4] for obtaining high-quality local optimum benchmark solutions. We remark that the FPLinQ benchmark solutions can also be utilized as training targets for supervised training of the neural network, and a numerical comparison is provided later in the paper. FPLinQ relies on a transformation of the SINR expression that decouples the signal and the interference terms and a subsequent coordinated ascent approach to find the optimal transmit power for all the links. The FPLinQ algorithm is closely related to the weighted minimum mean-square-error (WMMSE) algorithm for weighted sum-rate maximization [8]. For the scheduling task, FPLinQ quantizes the optimized power in a specific manner to obtain the optimized binary scheduling variables.

## III. DEEP LEARNING BASED LINK SCHEDULING FOR SUM-RATE MAXIMIZATION

We begin by exploring the use of deep neural network for scheduling, while utilizing only location information, under the sum-rate maximization criterion. The sum-rate maximization problem (i.e., with equal weights) is considerably simpler than weighted rate-sum maximization, because all the links have equal priority. We aim to use path-losses and the geographical locations information to determine which subset of links should be scheduled.

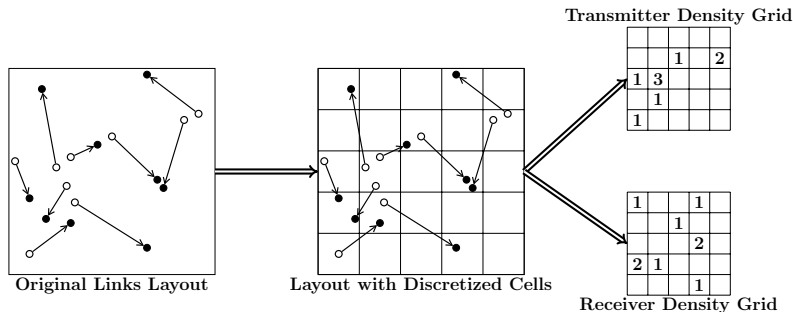


Fig. 1. Transmitter and receiver density grids

### A. Learning Based on Geographic Location Information

A central goal of this paper is to demonstrate that for wireless networks in which the channel gains are largely functions of distance dependent path-losses, the geographical location information is already sufficient as a proxy for optimizing link scheduling. This is in contrast to traditional optimization approaches for solving (2) that require the full instantaneous CSI, and also in contrast to the recent work [15] that proposes to use deep learning to solve the power control problem by learning the WMMSE optimization process. In [15], a fully connected neural network is designed that takes in the channel coefficient matrix as the input, and produces optimized continuous power variables as the output to maximize the sum rate. While satisfactory scheduling performance has been obtained in [15], the architecture of [15] is not scalable. In a D2D links network with  $N$  transmitter-receiver pairs, there are  $N^2$  channel coefficients. A fully connected neural network with  $N^2$  nodes in the input layer and  $N$  output layer would require at least  $O(N^3)$  interconnect weights (and most likely much more). Thus, the neural network architecture proposed in [15] has training and testing complexity that grows rapidly with the number of links.

Instead of requiring the full set of CSI between every transmitter and every receiver as the inputs to the neural network  $\{h_{ij}\}$ , which has  $O(N^2)$  entries, this paper proposes to use the geographic location information (GLI) as input, defined as a set of vectors  $\{(\mathbf{d}_i^{\text{tx}}, \mathbf{d}_i^{\text{rx}})\}_i$ , where  $\mathbf{d}_i^{\text{tx}} \in \mathbb{R}^2$  and  $\mathbf{d}_i^{\text{rx}} \in \mathbb{R}^2$  are the transmitter and the receiver locations of the  $i$ th link, respectively. Note that the input now scales linearly with the number of links, i.e.,  $O(N)$ .

We advocate using GLI as a substitute for CSI because in many wireless deployment scenarios, GLI already captures the main feature of channels: the path-loss and shadowing of a wireless link are mostly functions of distance and location. This is essentially true for outdoor wireless channels, and especially so in rural regions or remote areas, where the number of surrounding objects to reflect the wireless signals is sparse. An example application is a sensor network deployed outdoors for environmental monitoring purposes.

In fact, if we account for fast fading in addition, the CSI can be thought of as a stochastic function of GLI

$$\text{CSI} = f(\text{GLI}). \quad (3)$$

While optimization approaches to the wireless link scheduling problem aim to find a mapping  $g(\cdot)$  from CSI to the scheduling decisions, i.e.,

$$\mathbf{x} = g(\text{CSI}), \quad (4)$$

the deep learning architecture of this paper aims to capture directly the mapping from GLI to  $\mathbf{x}$ , i.e., to learn the function

$$\mathbf{x} = g(f(\text{GLI})). \quad (5)$$

### B. Transmitter and Receiver Density Grid as Input

To construct the input to the neural network based on GLI, we quantize the continuous  $(\mathbf{d}_i^{\text{tx}}, \mathbf{d}_i^{\text{rx}})$  in a grid form. Without loss of generality, we assume a square  $\ell \times \ell$  meters deployment area, partitioned into equal-size square cells with an edge length of  $\ell/M$ , so that there are  $M^2$  cells in total. We use  $(s, t) \in [1 : M] \times [1 : M]$  to index the cells. For a particular link  $i$ , let  $(s_i^{\text{tx}}, t_i^{\text{tx}})$  be the index of the cell where the transmitter  $\mathbf{d}_i^{\text{tx}}$  is located, and  $(s_i^{\text{rx}}, t_i^{\text{rx}})$  be the index of the cell where the receiver  $\mathbf{d}_i^{\text{rx}}$  is located. We use the tuple  $(s_i^{\text{tx}}, t_i^{\text{tx}}, s_i^{\text{rx}}, t_i^{\text{rx}})$  to represent the location information of the link.

We propose to construct two *density grid* matrices of size  $M \times M$ , denoted by  $T$  and  $R$ , to represent the density of the *active* transmitters and receivers, respectively, in the geographical area. The density grid matrices are constructed by simply counting the total number of active transmitters and receivers in each cell, as illustrated in Fig. 1. The activation pattern  $\{x_i\}$  is initialized as a vector of all 1's at the beginning. As the algorithm progressively updates the activation pattern, the density grid matrices are updated as

$$T(s, t) = \sum_{\{i | (s_i^{\text{tx}}, t_i^{\text{tx}}) = (s, t)\}} x_i, \quad (6)$$

$$R(s, t) = \sum_{\{i | (s_i^{\text{rx}}, t_i^{\text{rx}}) = (s, t)\}} x_i. \quad (7)$$

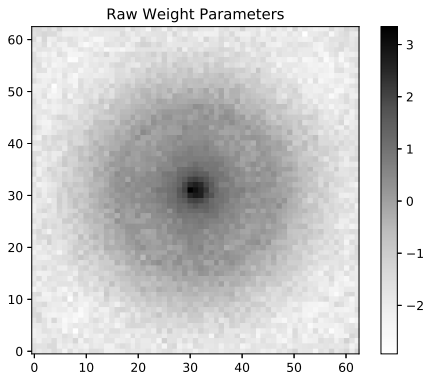


Fig. 2. A trained spatial convolution filter (in log scale)

### C. Novel Deep Neural Network Structure

The overall neural network structure for link scheduling with sum-rate objective is an iterative computation graph. A key novel feature of the network structure is a forward path including two stages: a convolution stage that captures the interference patterns of neighboring links based on the geographic location information and a fully connected stage that captures the nonlinear functional mapping of the optimized schedule. Further, we propose a novel *feedback connection* between the iterations to update the state of optimization. The individual stages and the overall network structure are described in detail below.

1) *Convolution Stage*: The convolution stage is responsible for computing two functions, corresponding to that of the interference each link causes to its neighbors and the interference each link receives from its neighbors, respectively. As a main innovation in the neural network architecture, we propose to use spatial convolutional filters, whose coefficients are optimized in the training process, that operate directly on the transmitter and receiver density grids described in the previous section. The transmitter and receiver spatial convolutions are computed in parallel on the two grids. At the end, two pieces of information are computed for the transmitter-receiver pair of each link: a convolution of spatial geographic locations of all the nearby receivers that the transmitter can *cause interference to*, and a convolution of spatial geographic locations of all the nearby transmitters that the receiver can *experience interference from*. The computed convolutions are referred to as  $\text{TxINT}_i$  and  $\text{RxINT}_i$ , respectively, for link  $i$ .

Since the idea is to estimate the effect of total interference each link causes to nearby receivers and effect of the total interference each link is exposed to, we need to exclude the link's own transmitter and receiver in computing the convolutions. This is done by subtracting the contributions each link's own transmitter and receiver in the respective convolution sum.

The convolution filter is a 2D square matrix with fixed

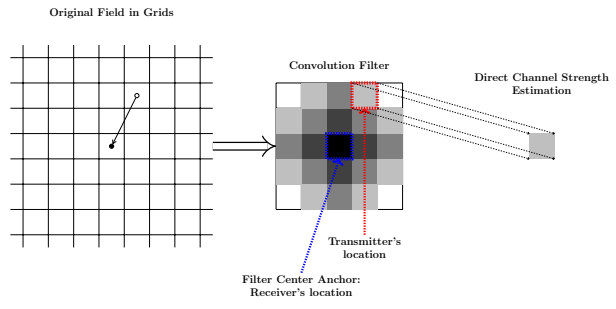


Fig. 3. Extracting direct channel strength from convolution filter

pre-defined size and trainable parameters. The value of each entry of the filter can be interpreted as the channel coefficient of a transceiver located at a specific distance from the center of the filter. Through training, the filter learns the channel coefficient by adjusting its weights. Fig. 2 shows a trained filter. As expected, the trained filter exhibits a circular symmetric pattern with radial decay.

The convolution stage described above summarizes two quantities for each link: the total interference produced by the transmitter and the total interference the receiver is being exposed to. Furthermore, we can also extract another important quantity for scheduling from the trained convolution filter: the *direct channel strength*. At the corresponding relative location of the transmitter from its receiver, the value of the convolution filter describes the channel gain of the direct link between this transmitter/receiver pair. The procedure for obtaining this direct channel strength is illustrated in Fig. 3. The direct channel strength is referred to as  $\text{DCS}_i$  for link  $i$ .

2) *Fully Connected Stage*: The fully connected stage is the second stage of the forward computation path, following the convolution stage described above. It takes a feature vector extracted for each link as input and produces an output  $x_i \in [0, 1]$ , (which can be interpreted as a relaxed scheduling variable or alternatively as continuous power) for that link.

The feature vector for each link comprises of the following entries:  $\text{TxINT}_i$ ,  $\text{RxINT}_i$ ,  $\text{DCS}_i$ ,  $\text{DCS}_{\max}$ ,  $\text{DCS}_{\min}$ ,  $x_i^{t-1}$ . The first three terms have been explained in the previous section.  $\text{DCS}_{\max}$  and  $\text{DCS}_{\min}$  denote the largest and smallest direct channel strength among links in the entire layout; and  $x_i^{t-1}$  represents the fully connected stage output at the previous iteration in the overall feedback structure, as described later. The tuple  $(\text{TxINT}_i, \text{RxINT}_i)$  describes the interference between the  $i$ th link and its neighbors, while the triplet  $(\text{DCS}_i, \text{DCS}_{\max}, \text{DCS}_{\min})$  describes the link's own channel strength as compared to the strongest and the weakest links in the entire layout.

It is worth noting that the minimum and maximum channel strengths over the layout are chosen here to characterize the range of the direct channel strengths. This is appropriate when the D2D link pairwise distances are roughly uniform, as we assume in the numerical simulations of this paper.

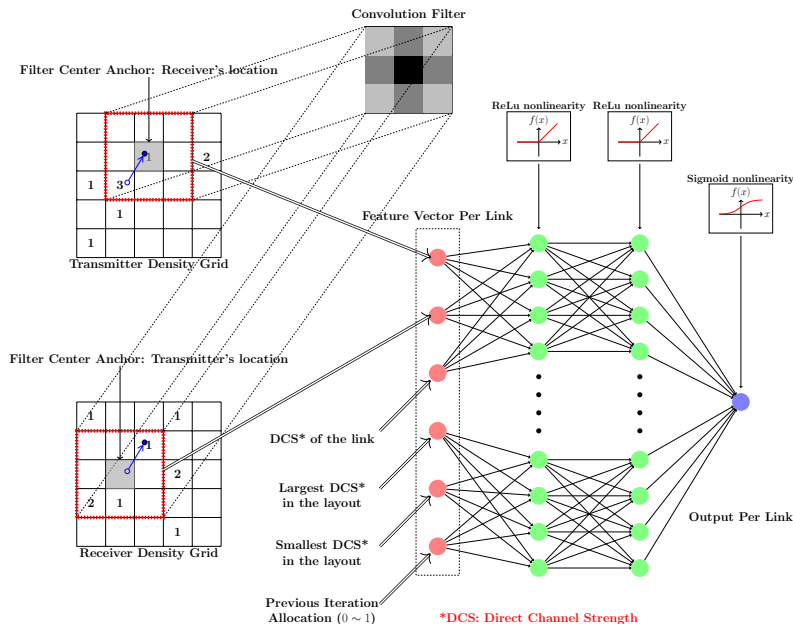


Fig. 4. Forward computation path for a single link with spatial convolutions and link distance as input to a neural network

However, if the D2D link pairwise distances do not follow a uniform distributions, a more robust characterization could be, for example, 10th and 90th percentile values of the channel strength distribution, to alleviate the effect of potential outliers.

The value  $x_i$  for this link is computed based on its feature vector through the functional mapping of a fully connected neural network (denoted here as  $F_{fc}$ ) over the feedback iterations indexed by  $t$ :

$$x_i^t \leftarrow F_{fc}(\text{TxINT}_i, \text{RxINT}_i, \text{DCS}_i, \text{DCS}_{\max}, \text{DCS}_{\min}, x_i^{t-1}). \quad (8)$$

The convolution stage and the fully connected stage together form one forward computation path for each transmitter-receiver pair, as depicted in Fig. 4. In the implementation, we use two hidden layers with 30 neurons in each layer to ensure sufficient expressive power of the neural network. A rectified linear unit (ReLU) is used at each neuron in the hidden layers; a sigmoid nonlinearity is used at the output node to produce a value in  $[0, 1]$ .

3) *Feedback Connection*: The forward computation (which includes the convolution stage and the fully connected stage) takes the link activation pattern  $x_i$  as the input for constructing the density grid. In order to account for the progressive (de)activation pattern of the wireless links through the iterations (i.e., each subsequent interference estimates need to be aware of the fact that the deactivated links no longer produce or are subject to interference), we propose a feedback structure, in which each iteration of the neural network takes the continuous output  $x$  from the previous iteration as input, then iterate for a fixed number of iterations. We find experimentally that the network is

then able to converge within a small number of iterations.

The feedback stage is designed as following: After the completion of  $(t - 1)$ th forward computation, the  $\mathbf{x}$  vector of  $[0, 1]$  values is obtained, with each entry representing the activation status for each of the  $N$  links. Then, a new forward computation is started with input density grids prepared by feeding this  $\mathbf{x}$  vector into (6)-(7). In this way, the activation status for all  $N$  links are updated in the density grids for subsequent interference estimations. Note that the trainable weights of the convolutional filter and the neural network are tied together over the multiple iterations for more efficient training.

After a fixed number of iterations, the scheduling decisions are obtained from the neural network by quantizing the  $\mathbf{x}$  vector from the last iteration into binary values, representing the scheduling decisions of the  $N$  links.

The overall feedback structure is depicted in Fig. 5. We emphasize here that the neural network is designed on a per-link basis, thus the overall model is scalable with respect to the network size. Specifically, at the convolution stage, the convolutions are computed based on the fixed (and trained) convolution filter that covers the neighboring non-negligible interference sources. At the fully connected stage, the neural networks of different links are decoupled, thus scheduling can be performed in a distributed fashion.

Moreover, in the training stage, the convolutional filter parameters and the neural network weights of the different links are tied together. This facilitates efficient training, and implicitly assumes that the propagation environments of the different links are similar. Under this homogeneity assumption, regardless of how large the layout is and how many links are to be scheduled in the network, the overall

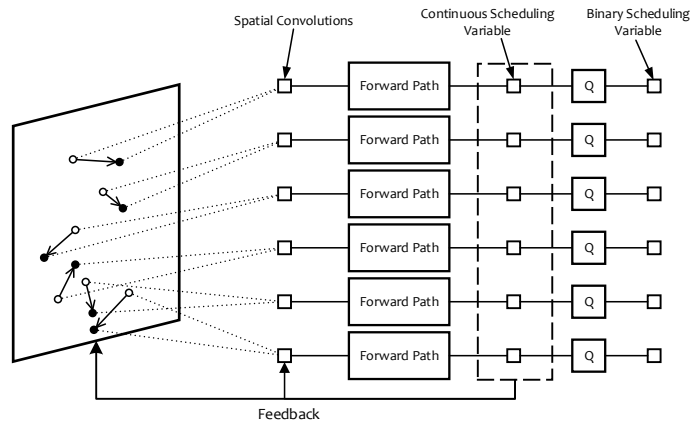


Fig. 5. Overall neural network with one forward path per link and with feedback connections and quantized output (denoted as “Q”).

trained neural network model can be directly utilized for scheduling, without adjustment or re-training,

#### D. Training Process

The overall deep neural network is trained using wireless network layouts with randomly located links and with the transmitter-receiver distances following a specific distribution. Specifically, we train the model to maximize the target sum rate via gradient descent on the convolutional filter weights and neural network weight parameters. It is worth noting that while the channel gains are needed at the training stage for computing rates, they are not needed for scheduling, which only requires GLI.

To allow the gradients to be back-propagated through the network, we do not discretize the network outputs when computing the rates. Therefore, the unsupervised training process is essentially performing a power control task for maximizing the sum rate. The scheduling decisions are obtained from discretizing the optimized power variables.

We randomly generate wireless D2D networks consisting of  $N = 50$  D2D pairs in a 500 meters by 500 meters region. The locations for the transmitters are generated uniformly within the region. The locations of the receivers are generated according to a uniform distribution within a pairwise distances of  $d_{\min} \sim d_{\max}$  meters from their respective transmitters. We generate 800,000 such network layouts for training.

The transmitter-receiver distance has significant effect on the achievable rate. Link scheduling for sum-rate maximization tends to favor short links over long links, so the distribution of the link distances has significant effect on the scheduling performance. To develop the capacity of the proposed deep learning approach to accommodate varying transmitter-receiver distances, we generate training samples based on the following distribution:

- Generate  $d_{\min}$  uniformly from  $2 \sim 70$  meters.
- Generate  $d_{\max}$  uniformly from  $d_{\min} \sim 70$  meters.
- Generate D2D links distance as uniform  $d_{\min} \sim d_{\max}$ .

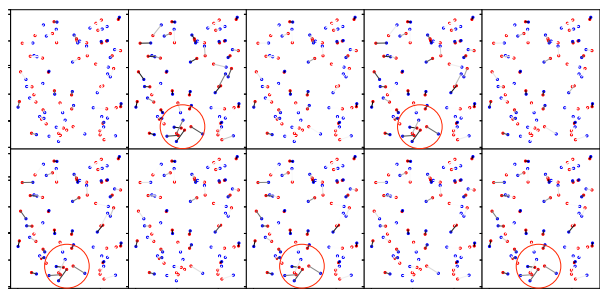


Fig. 6. Oscillatory behavior in the neural network training process.

As noted earlier, we could have also used a state-of-the-art optimization algorithm to generate locally optimal schedules as targets and train the neural network in a supervised fashion. Promising results have been obtained for specific transmitter-receiver distance distributions (e.g.,  $2 \sim 65$  meters) [21], but supervised learning does not always work well for more general distributions; see Section IV-E. A possible explanation is that the high quality local optimal schedules are often not smooth functional mappings of the network parameters, and are therefore difficult to learn.

#### E. Symmetry Breaking

The overall neural network is designed to encourage links to deactivate either when it produces too much interference to its neighbors, or when it experiences too much interference from its neighbors. However, because training happens in stages and all the links update their activation pattern in parallel, the algorithm frequently gets into situations in which multiple links may oscillate between being activated and deactivated.

Consider the following scenario involving two closely located links with identical surroundings. Starting from the initialization stage where both links are fully activated, both links see severe interference coming from each other. Thus, at the end of the first forward path, both links would be turned off. Now assuming that there are no other strong

TABLE I  
DESIGN PARAMETERS FOR THE SPATIAL DEEP NEURAL NETWORK

Parameters	Values	
Convolution Filter Size	63 cells $\times$ 63 cells	
Cell Size	5m by 5m	
First Hidden Layer	30 units	
Second Hidden Layer	30 units	
Number of Iterations	Training	3~20 iterations
	Testing	20 iterations

interference in the neighborhood, then at the end of the second iteration, both links would see little interference; consequentially both would be encouraged to be turned back on. This oscillation pattern can keep going, and the training process for the neural network would never converge to a good schedule (which is that one of the two links should be on). Fig. 6 shows a visualization of the phenomenon. Activation patterns produced by the actual training process are shown in successive snapshots. Notice that the three closely located strong interfering links located at middle bottom of the layout have the oscillating pattern between successive iterations. The network could not converge to an optimal scheduling where only one of the three links are scheduled. The same happens to the two links in the upper left part of the area.

To resolve this problem, a stochastic update mechanism to break the symmetry is proposed. At the end of each forward path, the output vector  $\mathbf{x}$  contains the updated activation pattern for all the links. However, instead of feeding back  $\mathbf{x}$  directly to the next iteration, we feedback the updated entries of  $\mathbf{x}$  with 50% probability (and feedback the old entries of  $\mathbf{x}$  with 50% probability). This symmetry breaking is used in both the training and testing phase and is observed to benefit the overall performance of the neural network.

#### IV. PERFORMANCE OF SUM-RATE MAXIMIZATION

##### A. Testing on Layouts of Same Size as Training Samples

We generate testing samples of random wireless D2D network layouts of the same number of links and the same size as the training samples, except with fixed uniform link distance distribution between some values of  $d_{\min}$  and  $d_{\max}$ . The channel model is adapted from the short-range outdoor model ITU-1411 with a distance-dependent path-loss [22], over 5MHz bandwidth at 2.4GHz carrier frequency, and with 1.5m antenna height and 2.5dBi antenna gain. The transmit power level is 40dBm; the background noise level is -169dBm/Hz. We assume an SNR gap of 6dB to Shannon capacity to account for practical coding and modulation.

For each specific layout and each specific channel realization, the FPLinQ algorithm [4] is used to generate the sum-rate maximizing scheduling output with a maximum iteration of 100. We note that although FPLinQ guarantees

TABLE II  
AVERAGE SUM RATE AS PERCENTAGE OF FP

%	CSI	30~70	2~65	10~50	all 30
Learning	$\times$	92.19	98.36	98.42	96.90
Greedy	$\checkmark$	84.76	97.08	94.00	84.56
Strongest	$\times$	59.66	82.03	75.41	N/A
Random	$\times$	35.30	47.47	49.63	50.63
All	$\times$	26.74	54.18	48.22	43.40
FP	$\checkmark$	100	100	100	100

monotonic convergence for the optimization over the continuous power variables, it does not necessarily produce monotonically increasing sum rate for scheduling. Experimentally, scheduling outputs after 100 iterations show good numerical performance. We generate 5000 layouts for testing in this section.

The design parameters for the neural network are summarized in the Table I. We compare the sum rate performance achieved by the trained neural network with each of the following benchmarks in term of both the average and the maximum sum rate over all the testing samples:

- **All Active:** Activate all links.
- **Random:** Schedule each link with 0.5 probability.
- **Strongest Links First:** We sort all links according to the direct channel strength, then schedule a fixed portion of the strongest links. The optimal percentage is taken as the average percentage of active links in the FP target.
- **Greedy:** Sort all links according to the link distance, then schedule one link at a time. Choose a link to be active only if scheduling this link strictly increases the objective function (i.e., the sum rate). Note that the interference at all active links needs to be re-evaluated in each step as soon as a new link is turned on or off.
- **FP:** Run FPLinQ for 100 iterations.

We run experiments with the following D2D links pairwise distance distributions in the test samples:

- Uniform in 30 ~ 70 meters.
- Uniform in 2 ~ 65 meters.
- Uniform in 10 ~ 50 meters.
- All links at 30 meters.

The distance distribution affects the optimal scheduling strategies, e.g., in how advantageous it is for scheduling only the strongest links. The sum rate performance of each of the above methods are reported in Table II. The performance is expressed as the percentages as compared to FPLinQ.

As shown in Table II, the proposed spatial learning approach always achieves more than 92% of the average sum rate produced by FPLinQ for all cases presented, *without explicitly knowing the channels*. The neural network also outperforms the greedy heuristic (which requires CSI) and outperforms other benchmarks by large margins.

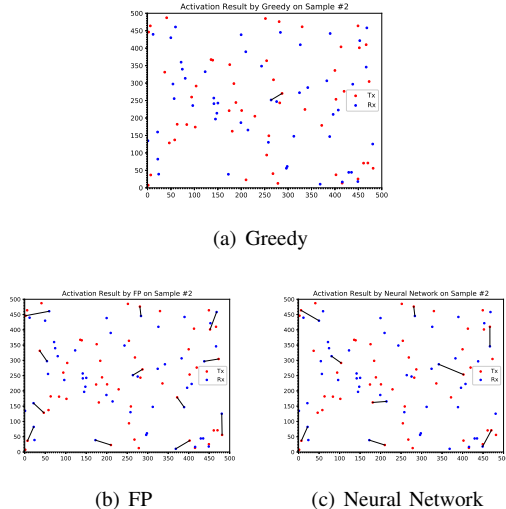


Fig. 7. Greedy heuristic prematurely activates the strongest link

The main reason that the greedy heuristics performs poorly is that it always activate the strongest link first, but once activated, the algorithm does not reconsider the scheduling decisions already made. The earlier scheduling decision may be suboptimal; this leads to poor performance as illustrated in an example in Fig. 7. Note that under the channel model used in simulation, the interference of an activated link reaches a range of 100m to 300m. If a greedy algorithm activates a link in the center of the 500m by 500m layout, it could preclude the activation of all other links, while the optimal scheduling should activate multiple weaker links roughly 100m to 300m apart as shown in Fig. 7.

Throughout testings of many cases, including the example shown in Fig. 7, the spatial learning approach always produces a scheduling pattern close to the FP output. This shows that the neural network is capable of learning the state-of-the-art optimization strategy.

### B. Generalizability to Arbitrary Topologies

An important test of the usefulness of the proposed spatial deep learning design is its ability to generalize to different layout dimensions and link distributions. Intuitively, the neural network performs scheduling based on an estimate of the direct channel and the aggregate interference from a local region surrounding the transmitter and the receiver of each link. Since both of these estimates are local, one would expect that the neural network should be able to extend to general layout.

To validate this generalization ability, we test the trained neural network on layouts with larger number of links, while first keeping the link density the same, then further test on layouts in which the link density is different. Note that we do not perform any further training on the neural network. For each test, 500 random layouts are generated to obtain the average maximum sum rate.

TABLE III  
GENERALIZABILITY TO LAYOUTS OF LARGER DIMENSIONS BUT SAME LINK DENSITY AND LINK DISTANCE: SUM RATE AS % OF FP

Size (m <sup>2</sup> )	Links	2m~65m		All 30m	
		DL	Greedy	DL	Greedy
750 × 750	113	98.5	102.4	98.4	98.4
1000 × 1000	200	99.2	103.2	98.3	98.8
1500 × 1500	450	99.5	103.8	98.3	100.0
2000 × 2000	800	99.7	104.1	98.8	100.8
2500 × 2500	1250	99.7	104.2	99.1	101.3

TABLE IV  
GENERALIZABILITY TO LAYOUTS WITH DIFFERENT LINK DENSITIES: SUM RATE AS % OF FP

Size (m <sup>2</sup> )	Links	2m~65m		All 30m	
		DL	Greedy	DL	Greedy
500 × 500	10	95.5	90.0	94.9	81.6
	30	97.0	93.2	96.1	81.3
	100	98.6	99.8	99.0	88.7
	200	97.8	101.7	96.0	92.4
	500	93.0	104.1	92.9 <sup>1</sup>	92.8

<sup>1</sup> 50 iterations are required for deep learning to achieve this result

1) *Generalizability to Layouts of Large Sizes*: First, we keep the link density and distance distribution the same and test the performance of the neural network on larger layouts occupying an area of up to 2.5km by 2.5km and 1250 links. The resulting sum rate performance is presented in Table III. Note that following the earlier convention, the entries for the deep learning (DL) neural network and greedy method are the percentages of sum rates achieved as compared with FP, averaged over the testing set.

Table III shows that the neural network is able to generalize to layouts of larger dimensions very well, with its performance very close to FP. It is worth emphasizing that while the greedy algorithm also performs well (likely because the phenomenon of Fig. 7 is less likely to occur on larger layouts), it requires CSI, as opposed to just location information utilized by spatial deep learning.

2) *Generalizability to Layouts with Different Link Densities*: We further explore the neural network's generalization ability in optimizing scheduling over layouts that have different link densities as compared to the training set. For this part of the evaluation, we fix the layout size to be 500 meters by 500 meters as in the training set, but instead of having 50 links, we vary the number of links in each layout from 10 to 500. The resulting sum rate performances of deep learning and the greedy heuristics are presented in Table IV.

As shown in Table IV, with up to 4-fold increase in the density of interfering links, the neural network is able to perform near optimally, achieving almost the optimal FP sum rate, while significantly outperforming the greedy algorithm, especially when the network is sparse.



TABLE V  
SUM RATE AS % OF FP ON CHANNELS WITH FAST FADING

%	CSI	30~70	2~65	10~50	30
DL	✗	71.8	88.6	82.5	73.9
FP no fade	✓	77.7	88.9	82.7	76.3
Greedy	✓	95.9	98.3	97.7	96.7
Strongest	✓	65.4	80.8	75.0	68.8
Random	✗	31.7	44.5	44.0	42.7
All Active	✗	25.3	50.4	43.8	38.4
FP	✓	100	100	100	100

However, the generalizability of deep learning does have limitations. When the number of links increases to 500 or more (10-fold increase as compared to training set), the neural network becomes harder to converge, resulting in dropping in performance. This is reflected in one entry in the last row of Table IV, where it takes 50 iterations for the neural network to reach a satisfactory rate performance. If the link density is further increased, it may fail to converge. Likely, new training set with higher link density would be needed.

### C. Sum Rate Optimization with Fast Fading

So far we have tested on channels with only a path-loss component (according to the ITU-1411 outdoor model). Since path-loss is determined by location, the channels are essentially deterministic function of the location.

In this section, Rayleigh fast fading is introduced into the testing channels. This is more challenging, because the channel gains are now stochastic functions of GLI inputs. Note that the neural network is still trained using channels without fading.

We use test layouts of 500 meters by 500 meters with 50 D2D links and with 4 uniform link distance distributions. The sum rate performance results are presented in Table V, with an additional benchmark:

- **FP without knowing fading:** Run FP based on the CSI without fast fading effect added in. This represents the best that one can do without knowing the fast-fading.

As shown in Table V, the performance of deep learning indeed drops significantly as compared to FP or Greedy (both of which require exact CSI). However, it is still encouraging to see the performance of neural network matches *FP without knowing fading*, indicating that it is already performing near optimally given that only GLI is available as inputs.

### D. Computational Complexity

In this section, we further argue that the proposed neural network has a computation complexity advantage as compared to the greedy or FP algorithms by providing a theoretical analysis and some experimental verification.

1) *Theoretical Analysis:* We first provide the complexity scaling for each of the methods as functions of the number of links  $N$ :

- **FPLinQ Algorithm:** Within each iteration, to update scheduling outputs and relevant quantities, the dominant computation includes matrix multiplication with the  $N \times N$  channel coefficient matrix. Therefore, the complexity per iteration is  $O(N^2)$ . Assuming that a constant number of iterations is needed for convergence, the total run-time complexity is then  $O(N^2)$ .
- **Greedy Heuristic:** The greedy algorithm makes scheduling decisions for each link sequentially. When deciding whether to schedule the  $i$ th link, it needs to compare the sum rate of all links that have been scheduled so far, with and without activating the new link. This involves re-computing the interference, which costs  $O(i)$  computation. As  $i$  ranges from 1 to  $N$ , the overall complexity of the greedy algorithm is therefore  $O(N^2)$ .
- **Neural Network** Let the discretized grid be of dimension  $K \times K$ , and the spatial filter be of dimension  $J \times J$ . Furthermore, let  $h_0$  denotes the size of input feature vector for fully connected stage, and let  $(h_1, h_2, \dots, h_n)$  denote the number of hidden units for each of the  $n$  hidden layers (note that the output layer has one unit). The total run-time complexity of the proposed neural network can be computed as:

$$\underbrace{K^2 \times J^2}_{\text{Convolution Stage}} + N \times \underbrace{(h_0 h_1 + \dots + h_{n-1} h_n + h_n)}_{\text{Fully Connected Stage per Pair}} \quad (9)$$

Thus, given a layout of fixed region size, the time complexity of neural network scales as  $O(N)$ .

2) *Experimental Verification:* In actual implementations, due to its ability to utilize parallel computation architecture, the run-time of the neural network can be even less than  $O(N)$ . To illustrate this point, we measure the total computation time of scheduling one layout of varying number of D2D links by using FP and greedy algorithms and by using the proposed neural network. The timing is conducted on a single desktop, with the hardware specifications as below:

- FP and Greedy: Intel CPU Core i7-8700K @ 3.70GHz
- Neural Network: Nvidia GPU GeForce GTX 1080Ti

To provide reasonable comparison of the running time, we select hardwares most suited for each of the algorithms. The implementation of the neural network is highly parallelizable; it greatly benefits from the parallel computation power of GPU. On the other hand, FP and greedy algorithms have strictly sequential computation flows, thus benefiting more from CPU due to its much higher clock speed. The CPU and GPU listed above are selected at about the same level of computation power and price point with regard to their respective classes.

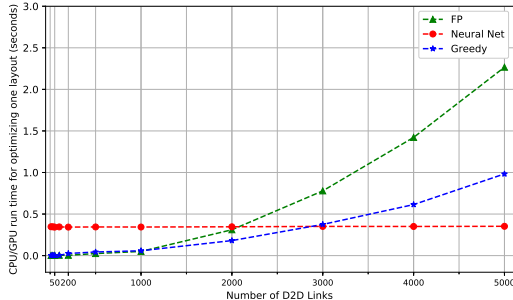


Fig. 8. Computation time on layouts with varying number of D2D links.

As illustrated in Fig. 8, the computational complexity of the proposed neural network is approximately constant, and is indeed several orders of magnitude less than FP baseline for layouts with large number of D2D links.

We remark here that the complexity comparison is inherently implementation dependent. For example, the bottleneck of our neural network implementation is the spatial convolutions, which are computed by built-in functions in TensorFlow [23]. The built-in function for computing convolution in TensorFlow, however, computes convolution in every location in the entire geographic area, which is an overkill. If a customized convolution operator is used only at specific locations of interests, the run-time complexity of our neural network can be further reduced. The complexity is expected to be  $O(N)$ , but with much smaller constant than the complexity curve in Fig. 8. We also remark that the computational complexity of traditional optimization approaches can potentially be reduced by further heuristics; see, e.g., [24].

To conclude, the proposed neural network has significant computational complexity advantage in large networks, while maintaining near-optimal scheduling performance. This is remarkable considering that the neural network has only been trained on layouts with 50 links, and requires only  $O(N)$  GLI rather than  $O(N^2)$  CSI.

### E. Unsupervised vs. Supervised Training

As mentioned earlier, the neural network can also be trained in a supervised fashion using the locally optimal schedule from FP, or in an unsupervised fashion directly using the sum-rate objective. Table VI compares these two approaches on the layouts of 500 meters by 500 meters with 50 D2D links, but with link distances following four different distributions. It is interesting to observe that while supervised learning is competitive for link distance distribution of 2m~65m, it generally has inferior performance in other cases. An intuitive reason is that when the layouts contain very short links, the sum-rate maximization scheduling almost always chooses these short links. It is easier for the neural network to learn such pattern in either a supervised or unsupervised fashion.

TABLE VI  
UNSUPERVISED VS. SUPERVISED TRAINING – SUM RATE AS % OF FP

Sum Rate (%)	2~65	10~50	30~70	30
Unsupervised	98.4	98.4	92.2	96.9
Supervised	96.2	90.3	83.2	82.0

When the layouts contain links of similar distances, many distinct local optima emerge, which tend to confuse the supervised learning process. In these cases, using the sum-rate objective directly tends to produce better results.

## V. SCHEDULING WITH PROPORTIONAL FAIRNESS

This paper has thus far focused on scheduling with sum-rate objective, which does not include a fairness criterion, thus tends to favor shorter links and links that do not experience large amount of interference. Practical applications of scheduling, on the other hand, almost always requires fairness. In the remaining part of this paper, we first illustrate the challenges in incorporating fairness in spatial deep learning, then offer a solution that takes advantage of the existing sum-rate maximization framework to provide fair scheduling across the network.

### A. Proportional Fairness Scheduling

We can ensure fairness in link scheduling by defining an optimization objective of a network utility function over the long-term average rates achieved by the D2D links. The long-term average rate, for example, can be defined over a duration of  $T$  time slots, with an exponential weighted window:

$$\bar{R}_i^t = (1 - \alpha)\bar{R}_i^{t-1} + \alpha R_i^t \quad t \leq T \quad (10)$$

where  $R_i^t$  is the instantaneous rate achieved by the D2D link  $i$  in time slot  $t$ , which can be computed as in (1) based on the scheduling decision binary vector in each time slot,  $\mathbf{x}^t$ . Define a concave and non-decreasing utility function  $U(\bar{R}_i)$  for each link. The network utility maximization problem is that of maximizing

$$\sum_{i=1}^N U(\bar{R}_i). \quad (11)$$

In the proportional fairness scheduling, the utility function is chosen to be  $U(\cdot) = \log(\cdot)$ .

The idea of proportional fairness scheduling is to maximize the quantity defined in (11) *incrementally* [25]. Assuming large  $T$ , in each new time slot, the incremental contribution of the achievable rates of the scheduled links to the network utility is approximately equivalent to a weighted sum rate [20]

$$\sum_{i=1}^N w_i R_i^t \quad (12)$$

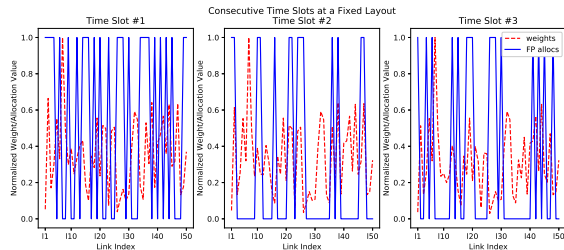


Fig. 9. The optimal scheduling can drastically change over slow varying proportional fairness weights

where the weights are set as:

$$w_i = \left. \frac{\partial U(\bar{R}_i^t)}{\partial R} \right|_{\bar{R}_i^t} = \left. \frac{\partial \log(\bar{R}_i^t)}{\partial R} \right|_{\bar{R}_i^t} = \frac{1}{\bar{R}_i^t}. \quad (13)$$

Thus, the original network utility maximization problem (11) can be solved by a series of weighted sum-rate maximization, where the weights are updated in each time slot as in (13). The mathematical equivalence of decomposition (11) to this series of weighted sum-rate maximization (12)-(13) is established in [26]. In the rest of the paper, to differentiate the weights in the weighted rate-sum maximization from the weights in the neural network, we refer  $w_i$  as the *proportional fairness weights*.

The weights  $w_i$  can take on any positive real values. This presents a significant challenge to deep learning based scheduling. In theory, one could train a different neural network for each set of weights, but the complexity of doing so would be prohibitive. To incorporate  $w_i$  as an extra input to the neural network turns out to be quite difficult as well. We explain this point in the next section, then offer a solution.

### B. Challenge in Learning to Maximize Weighted Sum Rate

A natural idea is to incorporate the proportional fairness weights as an extra input for each link in the neural network. However, this turns out to be quite challenging. We have implemented both the spatial convolution based neural network (using the structure mentioned in the first part of the paper, while taking an extra proportional fairness weight parameter) and the most general fully connected neural network to learn the mapping from the proportional fairness weights to the optimal scheduling. With millions of training data, the neural network is unable to learn such a mapping, even for a single fixed layout.

The essential difficulty lies in the high dimensionality of the function mapping. To visualize this complexity, we provide a series of plots of proportional fairness weights against FP scheduling allocations in sequential time slots in Fig. 9. It can be observed that the FP schedule can change drastically when the proportional weights only vary by a small amount. This is indeed a feature of proportional fairness scheduling: an unscheduled link sees its average rate decreasing and its proportional fairness

weight increasing over time until they cross a threshold, then all the sudden it gets scheduled. Thus, the mapping between the proportional fairness weights and the optimal schedule is highly sensitive to these sharp turns. If we desire to learn this mapping from a data-driven approach, one should expect to need a considerably larger amount of training samples to be collected just to be able to survey the functional landscape, not to mention the many more local sharp optima that would make training difficult. Further exacerbating the difficulty is the fact that there is no easy way to sample the space of proportional fairness weights. In a typical scheduling process, the sequence of weights are highly non-uniform.

### C. Weighted Sum Rate Maximization via Binary Weights

To tackle the proportionally fair scheduling problem, this paper proposes the following new idea: Since the neural network proposed in the first part of this paper is capable of generalizing to arbitrary topologies for sum-rate maximization, we take advantage of this ability by emulating weighted sum-rate maximization by sum-rate maximization, but over a judiciously chosen subset of links.

The essence of scheduling is to select an appropriate subset of users to activate. Our idea is therefore to first construct a shortlist of candidate links based on the proportional fairness weights alone, then further refine the candidate set of links using deep learning. Alternatively, this can also be thought of as to approximate the proportional fairness weights by a binary weight vector taking only the values of 0 or 1.

The key question is how to select this initial shortlist of candidate links, or equivalently how to construct the binary weight vector. Denote the original proportional fairness weights as described in (13) by  $\mathbf{w}^t$ . Obviously, the links with higher weights should have higher priority. The question is how many of the links with the large weights should be included.

This paper proposes to include the following subset of links. We think of the problem as to approximate  $\mathbf{w}^t$  by a binary 0-1 vector  $\hat{\mathbf{w}}^t$ . The proposed scheme finds this binary approximation in such a way so that the dot product between  $\mathbf{w}^t$  (normalized to unit  $\ell_2$ -norm) and  $\hat{\mathbf{w}}^t$  (also normalized) is maximized. For a fixed real-valued weight vector  $\mathbf{w}^t$ , we find the binary weight vector  $\hat{\mathbf{w}}^t$  as follows:

$$\hat{\mathbf{w}}^t = \arg \min_{\mathbf{y} \in \{0,1\}^N} \left\langle \frac{\mathbf{y}}{\|\mathbf{y}\|_2}, \frac{\mathbf{w}^t}{\|\mathbf{w}^t\|_2} \right\rangle \quad (14)$$

where  $\langle \cdot, \cdot \rangle$  denotes the dot product of two vectors. Geometrically, this amounts to finding an  $\hat{\mathbf{w}}^t$  that is closest to  $\mathbf{w}^t$  in term of the angle between the two vectors.

Algorithmically, such a binary vector can be easily found by first sorting the entries of  $\mathbf{w}^t$ , then setting the largest  $k$  entries to 1 and the rest of 0, where  $k$  is found by a linear search using the objective function in (14). With the binary weight vector  $\hat{\mathbf{w}}^t$ , the weighted sum rate optimization

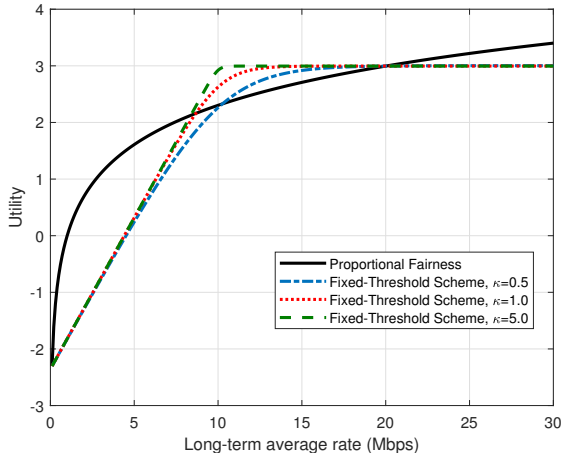


Fig. 10. Utility function of the fixed-threshold binary weighting scheme vs. proportional fairness scheduling. Here  $\theta = 0.1$ .

is effectively reduced to sum rate optimization, over the subset of links with weights equal to 1. We can then utilize spatial deep learning to perform scheduling over this subset of links.

#### D. Utility Analysis of Binary Reweighting Scheme

The proposed binary reweighting scheme is a heuristic for producing fair user scheduling, but a rigorous analysis of such a scheme is challenging. In the following, we provide a justification as to why such a scheme provides fairness. From a stochastic approximation perspective [26], the proposed way of updating the weights can be thought of as maximizing a particular utility function of the long-term average user rate. To see what this utility function looks like, we start with a simple fixed-threshold scheme:

$$\hat{w}_i = \begin{cases} 1, & \text{if } w_i \geq \theta \\ 0, & \text{otherwise} \end{cases} \quad (15)$$

for some fixed threshold  $\theta > 0$ , where  $\hat{w}_i$  and  $w_i$  are the binary weight and the original weight, respectively. Since  $w_i = 1/\bar{R}_i$ , we can rewrite (15) as

$$\hat{w}_i = \begin{cases} 1, & \text{if } \bar{R}_i \leq \frac{1}{\theta} \\ 0, & \text{otherwise} \end{cases}. \quad (16)$$

Recognizing (16) as a reverse step function with sharp transition from 1 to 0 at  $1/\theta$ , we propose to use the following *reverse sigmoid* function to mimic  $\hat{w}_i$ :

$$W(\bar{R}_i) = \frac{1}{1 + \exp(\kappa(\bar{R}_i - \theta))} \quad (17)$$

where the parameter  $\kappa > 0$  controls the steepness of the  $W(\bar{R}_i)$ . We can now recover the utility function that the reweighting scheme (17) implicitly maximizes.

For a fixed strictly concave utility  $U(\bar{R}_i)$ , the user weights are set as  $w_i = U'(\bar{R}_i)$ . Thus, given some

reweighting scheme  $w_i = U'(\bar{R}_i)$ , the corresponding utility objective must be  $U(\bar{R}_i)$ . In our case, the utility function  $U(\bar{R}_i)$  can be computed explicitly as

$$\begin{aligned} U(\bar{R}_i) &= \alpha \int W(\bar{R}_i) d\bar{R}_i \\ &= \alpha \bar{R}_i - \frac{\alpha}{\kappa} \ln(1 + \exp(\kappa(\bar{R}_i - \theta))) + \beta \end{aligned} \quad (18)$$

where  $\alpha > 0$  is a scaling parameter and  $\beta \in \mathbb{R}$  is an offset parameter. These two parameters do not affect the scheduling performance. Fig. 10 compares the utility function  $U(\bar{R}_i)$  of the binary weighting scheme with the log-utility proportional fairness function. It is observed that the utility of the fixed-threshold scheme follows the same trend as the proportional fairness utility.

Note that the above simplified analysis assumes that the threshold  $\theta$  is fixed, but in the proposed binary reweighting scheme, the threshold changes adaptively in each step, so this analysis is an approximation. Observe also that the utility function of the binary reweighting scheme saturates when  $\bar{R}$  is greater than the threshold, in contrast to the proportional fairness utility which grows logarithmically with  $\bar{R}$ . This difference becomes important in the numerical evaluation of the proposed scheme.

## VI. PERFORMANCE OF PROPORTIONAL FAIRNESS SCHEDULING

We now evaluate the performance of the deep learning based approach with binary reweighting for proportional fairness scheduling in three types of wireless network layouts:

- The layouts with the same size and link density;
- The larger layouts but with same link density;
- The larger layouts but with different link density.

For testing on layouts with the same setting, 20 distinct layouts are generated for testing, with each layout being scheduled over 500 time slots. For the other two settings, 10 distinct layouts are generated and scheduled over 500 time slots. Since scheduling is performed here within a finite number of time slots, we compute the mean rate of each link by averaging the instantaneous rates over all the time slots:

$$\bar{R}_i = \frac{1}{T} \sum_{t=1}^T R_i^t. \quad (19)$$

The utility of each link is computed as the logarithm of the mean rates in Mbps. The network utility is the sum of link utilities as defined in (11). The utilities of distinct layouts are averaged and presented below. To further illustrate the mean rate distribution of the D2D link, we also plot the cumulative distribution function (CDF) of the mean link rates, serving as a visual illustration of fairness.

The proposed deep learning based proportional fairness scheduling solves a sum-rate maximization problem over a subset of links using the binary reweighting scheme in each

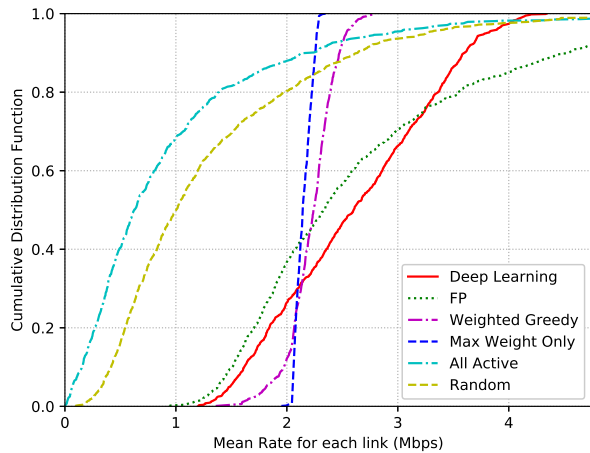


Fig. 11. CDF of mean rates for layouts of 50 links in 500m $\times$ 500m area for the case that link distance distribution is 30m to 70m.

TABLE VII  
MEAN LOG UTILITY PERFORMANCE FOR PROPORTIONALLY FAIR SCHEDULING

	CSI	30-70	2-65	10-50	30
DL	$\times$	45.9	61.9	63.3	62.6
W. Greedy	$\checkmark$	39.7	51.5	51.1	49.0
Max Weight	$\times$	38.3	42.1	41.9	41.4
Random	$\times$	0.76	38.4	38.7	35.1
All Active	$\times$	-27.6	24.0	20.9	15.7
FP	$\checkmark$	45.2	63.1	63.3	63.0

time slot. In addition to the baseline schemes mentioned previously, we also include:

- **Max Weight:** Schedule the single link with the highest proportional fairness weight in each time slot.
- **Weighted Greedy:** Generate a fixed ordering of all links by sorting all the links according to the proportional fairness weight of each link multiplied by the maximum direct link rate it can achieve without interferences, then schedule one link at a time in this order. Choose a link to be active only if scheduling this link strictly increases the weighted sum rate. Note that interference is taken into account when computing the link rate in the weighted sum rate computation. Thus, CSI is required. In fact, the interference at all active links needs to be re-evaluated in each step whenever a new link is activated.

1) *Performance on Layouts of Same Size and Link Density:* In this first case, we generate testing layouts with size 500 meters by 500 meters, with 50 D2D links in each layout. Similar to sum rate optimization evaluation, we have conducted the testing under the following 4 D2D links pairwise distance distributions:

- Uniform in 30 ~ 70 meters.
- Uniform in 2 ~ 65 meters.

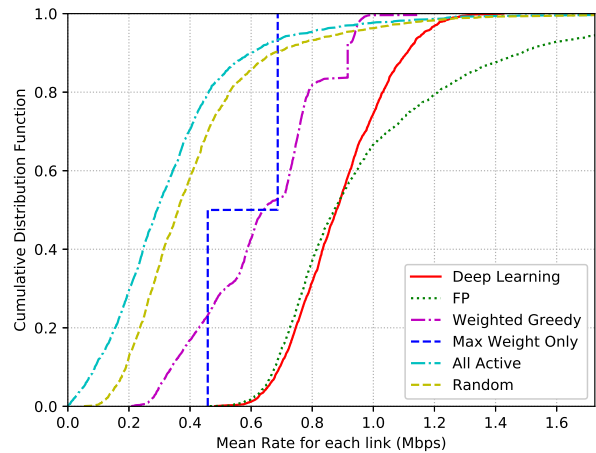


Fig. 12. CDF for mean rates of Layouts with 200 links in 500m $\times$ 500m area with link distance fixed at 30m

- Uniform in 10 ~ 50 meters.
- All 30 meters.

The log utility values achieved by the various schemes are presented in Table VII. The CDF plot of mean rates achieved for the case of link distributed in 30m-70m is presented in Fig. 11.

Remarkably, despite the many approximations, the deep learning approach with binary reweighting achieves excellent log-utility values as compared to the FP. Its log-utility also exceeds the weighted greedy algorithm noticeably. We again emphasize that this is achieved with geographic information only without explicit CSI.

It is interesting to observe that the deep learning approach has a better CDF performance as compared to the FP in the low-rate regime, but worse mean rate beyond the 80-percentile range. This is a consequence of the fact that the implicit network utility function of the binary reweighting scheme is higher than proportional fairness utility at low rates, but saturates at high rate, as shown in Fig. 10.

2) *Performance on Larger Layouts with Same Link Density:* To demonstrate the ability of the neural network to generalize to layouts of larger size under the proportional fairness criterion, we conduct further testing on larger layouts with the same link density. We again emphasize that no further training is conducted. We test the following two D2D links pairwise distance distributions:

- Uniform in 2 ~ 65 meters.
- All 30 meters.

The results for this setting are summarized in Table VIII.

It is observed that under the proportional fairness criterion, the spatial deep learning approach still generalizes really well. It is competitive with respect to both FP and the weighted greedy methods, using only  $O(N)$  GLI as input and using the binary weight approximation.

TABLE VIII  
MEAN LOG UTILITY PERFORMANCE FOR PROPORTIONALLY FAIR SCHEDULING ON LARGER LAYOUTS WITH SAME LINK DENSITY

Layout Size	Links	2m~65m			all 30 m		
		FP	DL	W. Greedy	FP	DL	W. Greedy
750m × 750m	113	127	124	106	127	126	111
1000m × 1000m	200	217	205	203	219	214	205
1500m × 1500m	450	462	432	454	466	448	462

TABLE IX  
MEAN LOG UTILITY PERFORMANCE FOR PROPORTIONALLY FAIR SCHEDULING ON LAYOUTS WITH DIFFERENT LINK DENSITY

Layout Size	Links	2m~65m			all 30m		
		FP	DL	W. Greedy	FP	DL	W. Greedy
500m × 500m	30	52	49	47	50	50	44
	200	-11	-13	-90	-11	-26	-102
	500	-511	-514	-736	-485	-542	-739

3) *Performance on Layout with Different Link Density:* We further test the neural network on a more challenging case: layouts with different link densities than the setting on which it is trained. Specifically, we experiment on layouts of 500 meters by 500 meters size and varying number of D2D links. The resulting sum log utility value, averaged over 10 testing layouts, are summarized in Table IX.

It is observed that the neural network still competes really well against FP in log utility, and outperforms the weighted greedy method significantly. To visualize, we select one specific layout of 500 meters by 500 meters region with 200 links with link distances fixed to 30 meters, and provide the CDF plot of long-term mean rates achieved by each link in Fig. 12.

## VII. CONCLUSION

Deep neural network has had remarkable success in many machine learning tasks, but the ability of deep neural networks to learn the outcome of large-scale discrete optimization is still an open research question. This paper provides evidence that for the challenging scheduling task for the wireless D2D networks, deep learning can perform very well for sum-rate maximization. In particular, this paper demonstrates that in certain network environments, by using a novel geographic spatial convolution for estimating the density of the interfering neighbors around each link and a feedback structure for progressively adjusting the link activity patterns, a deep neural network can in effect learn the network interference topology and perform scheduling to near optimum based on the geographic spatial information alone, thereby eliminating the costly channel estimation stage.

Furthermore, this paper demonstrates the generalization ability of the neural network to larger layouts and to layouts of different link density (without the need for any further training). This ability to generalize provides computational complexity advantage for the neural network

on larger wireless networks as compared to the traditional optimization algorithms and the competing heuristics.

Moreover, this paper proposes a binary reweighting scheme to allow the weighted sum-rate maximization problem under the proportional fairness scheduling criterion to be solved using the neural network. The proposed method achieves near optimal network utility, while maintaining the advantage of bypassing the need for CSI.

Taken together, this paper shows that deep learning is promising for wireless network optimization tasks, especially when the models are difficult or expensive to obtain and when computational complexity of existing approaches is high. In these scenarios, a carefully crafted neural network topology specifically designed to match the problem structure can be competitive to the state-of-the-art methods.

## REFERENCES

- [1] Y. LeCun, L. Bottou, Y. Bengio, and P. Haffner, "Gradient-based learning applied to document recognition," *Proc. IEEE*, vol. 86, no. 11, pp. 2278–2324, Nov. 1998.
- [2] Y. LeCun, Y. Bengio, and G. Hinton, "Deep learning," *Nature*, pp. 436–444, May 2015.
- [3] K. Hornik, "Multilayer feedforward networks are universal approximators," *Neural Netw.*, vol. 2, pp. 359–366, 1989.
- [4] K. Shen and W. Yu, "FPLinQ: A cooperative spectrum sharing strategy for device-to-device communications," in *IEEE Int. Symp. Inf. Theory (ISIT)*, Jun. 2017, pp. 2323–2327.
- [5] —, "Fractional programming for communication systems—Part I: Power control and beamforming," *IEEE Trans. Signal Process.*, vol. 66, no. 10, pp. 2616–2630, May 15, 2018.
- [6] —, "Fractional programming for communication systems—Part II: Uplink scheduling via matching," *IEEE Trans. Signal Process.*, vol. 66, no. 10, pp. 2631–2644, May 15, 2018.
- [7] X. Wu, S. Tavildar, S. Shakkottai, T. Richardson, J. Li, R. Laroia, and A. Jovicic, "FlashLinQ: A synchronous distributed scheduler for peer-to-peer ad hoc networks," *IEEE/ACM Trans. Netw.*, vol. 21, no. 4, pp. 1215–1228, Aug. 2013.
- [8] Q. Shi, M. Razaviyayn, Z.-Q. Luo, and C. He, "An iteratively weighted MMSE approach to distributed sum-utility maximization for a MIMO interfering broadcast channel," *IEEE Trans. Signal Process.*, vol. 59, no. 9, pp. 4331–4340, Apr. 2011.

- [9] N. Naderializadeh and A. S. Avestimehr, "ITLinQ: A new approach for spectrum sharing in device-to-device communication systems," *IEEE J. Sel. Areas Commun.*, vol. 32, no. 6, pp. 1139–1151, Jun. 2014.
- [10] X. Yi and G. Caire, "Optimality of treating interference as noise: A combinatorial perspective," *IEEE Trans. Inf. Theory*, vol. 62, no. 8, pp. 4654–4673, Jun. 2016.
- [11] B. Zhuang, D. Guo, E. Wei, and M. L. Honig, "Scalable spectrum allocation and user association in networks with many small cells," *IEEE Trans. Commun.*, vol. 65, no. 7, pp. 2931–2942, Jul. 2017.
- [12] I. Rhee, A. Warriar, J. Min, and L. Xu, "DRAN: Distributed randomized TDMA scheduling for wireless ad hoc networks," *IEEE Trans. Mobile Comput.*, vol. 8, no. 10, pp. 1384–1396, Oct. 2009.
- [13] L. P. Qian and Y. J. Zhang, "S-MAPEL: Monotonic optimization for non-convex joint power control and scheduling problems," *IEEE Trans. Wireless Commun.*, vol. 9, no. 5, pp. 1708–1719, May 2010.
- [14] M. Johansson and L. Xiao, "Cross-layer optimization of wireless networks using nonlinear column generation," *IEEE Trans. Wireless Commun.*, vol. 5, no. 2, pp. 435–445, Feb. 2006.
- [15] H. Sun, X. Chen, Q. Shi, M. Hong, X. Fu, and N. D. Sidiropoulos, "Learning to optimize: Training deep neural networks for interference management," *IEEE Trans. Signal Process.*, vol. 66, no. 20, pp. 5438–5453, Aug. 2018.
- [16] M. Eisen, C. Zhang, L. F. O. Chamon, D. D. Lee, and A. Ribeiro, "Learning optimal resource allocations in wireless systems," [Online] Available: <https://arxiv.org/pdf/1807.08088>.
- [17] F. Liang, C. Shen, and F. Wu, "Power control for interference management via ensembling deep neural networks," 2018, preprint. [Online] Available: <https://arxiv.org/pdf/1807.10025>.
- [18] J. G. D. Forney and G. Ungerboeck, "Modulation and coding for linear gaussian channels," *IEEE Trans. Inf. Theory*, vol. 44, no. 6, Oct. 1998.
- [19] M. J. Neely, *Stochastic Network Optimization with Application to Communication and Queueing Systems*. Morgan & Claypool, 2010.
- [20] J. Huang, R. Berry, and M. Honig, "Distributed interference compensation for wireless networks," *IEEE J. Sel. Areas Commun.*, vol. 24, no. 5, pp. 1074–1084, May 2006.
- [21] W. Cui, K. Shen, and W. Yu, "Spatial deep learning in wireless scheduling," in *IEEE Global Commun. Conf. (GLOBECOM)*, Abu Dhabi, UAE, Dec. 2018.
- [22] *Recommendation ITU-R P.1411-8*. International Telecommunication Union, 2015.
- [23] M. Abadi *et al.*, "TensorFlow: Large-scale machine learning on heterogeneous systems," 2015, software available from tensorflow.org. [Online]. Available: <https://www.tensorflow.org/>
- [24] Z. Zhou and D. Guo, "1000-cell global spectrum management," in *ACM Int. Symp. Mobile Ad Hoc Netw. Comput. (MobiHoc)*, Jul. 2017.
- [25] E. F. Chaponniere, P. J. Black, J. M. Holtzman, and D. N. C. Tse, "Transmitter directed code division multiple access system using path diversity to equitably maximize throughput," U.S. Patent 345 700, Jun. 30, 1999.
- [26] H. J. Kushner and P. A. Whiting, "Convergence of proportional-fair sharing algorithms under general conditions," *IEEE Trans. Wireless Commun.*, vol. 3, no. 4, pp. 1250–1259, Jul. 2004.